Sparsity Promoting Variational Downscaling, Data fusion and Assimilation

Mohammad Ebtehaj [a,b] , Efi Foufoula-Georgiou [a]

a., Department of Civil Engineering, Saint Anthony Falls Laboratory and National Center for Earth-Surface Dynamics, University of Minnesota, USA
b., School of Mathematics, Minnesota Center for Industrial Mathematics, University of Minnesota, USA

UNIVERSITY OF MINNESOTA
Driven to Discover℠

Goal and Motivation

❑ Goals

- To develop state of the art algorithms for DOWNSCALING, FUSION, RETRIEVAL and ASSIMILATION of the non-Gaussian multi-sensor geophysical observations via SPARSE REPRESENTATION and NON-SMOOTH CONVEX OPTIMIZATION.

❑ Motivation:

- As multi-sensor geophysical data will be available routinely from multiple ground-based and spaceborne sensors, the need for new classes of estimators with less uncertainty becomes imperative for hydro-meteorological applications.
- Many geophysical signals are sparse in an appropriately chosen basis (e.g., wavelet, Fourier). In other words, a large number of expansion coefficients are near zero while a small number of them are significantly non-zero, carrying the energy and information content of the geophysical signal.
- The observed sparsity and recent developments in non-smooth convex optimization promise new classes of non-linear estimation algorithms which outperform the classic least squares (LS) methods. These new estimators can effectively capture potential singularities and abrupt transitions in geophysical states of interest.

Sparsity a Ubiquitous Signature

❑ a Probability Model

- Geophysical signals often exhibit sparsity in a pre-selected basis. In other words, expanding the geophysical signal of interest in an appropriately chosen domain, a large number of expansion coefficients are (near)-zero while a small number remains significantly non-zero. Distribution of the expansion coefficients are typically symmetric with heavier tail than the Gaussian case which can be well parameterized by the family of Generalized Gaussian distributions.

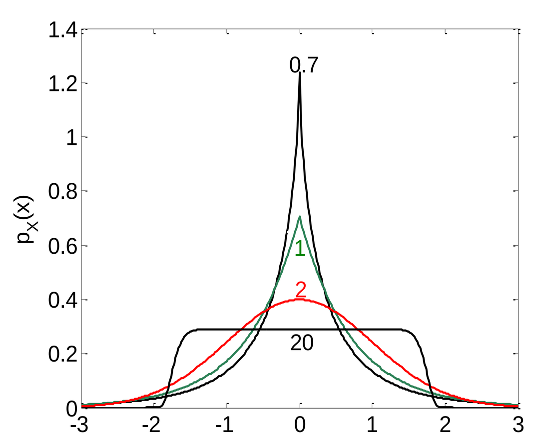

$$p(x) \propto \exp(-\lambda |x|^p)$$

Fig.1 Generalized Gaussian Distribution (GGD) spans a probability continuum from Delta Dirac (p=0) to a uniform density (p→∞). The Gaussian (p=2) and Laplace (p=1) densities are special cases.

❑ Sparsity of Geophysical Signals in the Wavelet Domain

- Many geophysical signals are intermittent. In other words, they suffer from frequent jumps and isolated singularities, followed by relatively calm periods of low activity and variability. These type of geophysical signals typically exhibit a sparse representation in the wavelet domain.
- **Rainfall Images:** Rainfall reflectivity images exhibit remarkable sparsity in the wavelet domain.

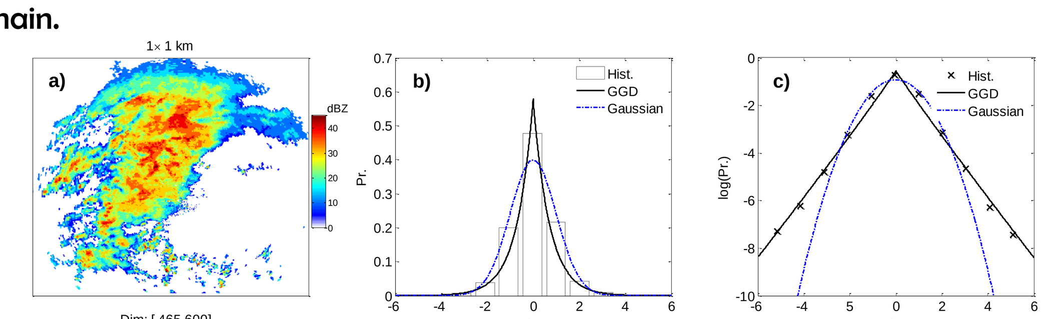

Fig.2 Evidence of heavy tailed distribution and sparsity of precipitation in the wavelet domain, (a) A ground-based radar rainfall reflectivity snapshot (1×1 km) over Houston, TX on 1998/11/13 (00:02:00 UTC). (b) Probability histogram of the horizontal derivatives (wavelet coefficients); solid line: fitted Generalized Gaussian density with $\lambda = 0.9$; and broken line: Gaussian density for comparison. The log-probability histogram in (c) contrasts the heavy tailed structure of precipitation derivatives versus the Gaussian distribution

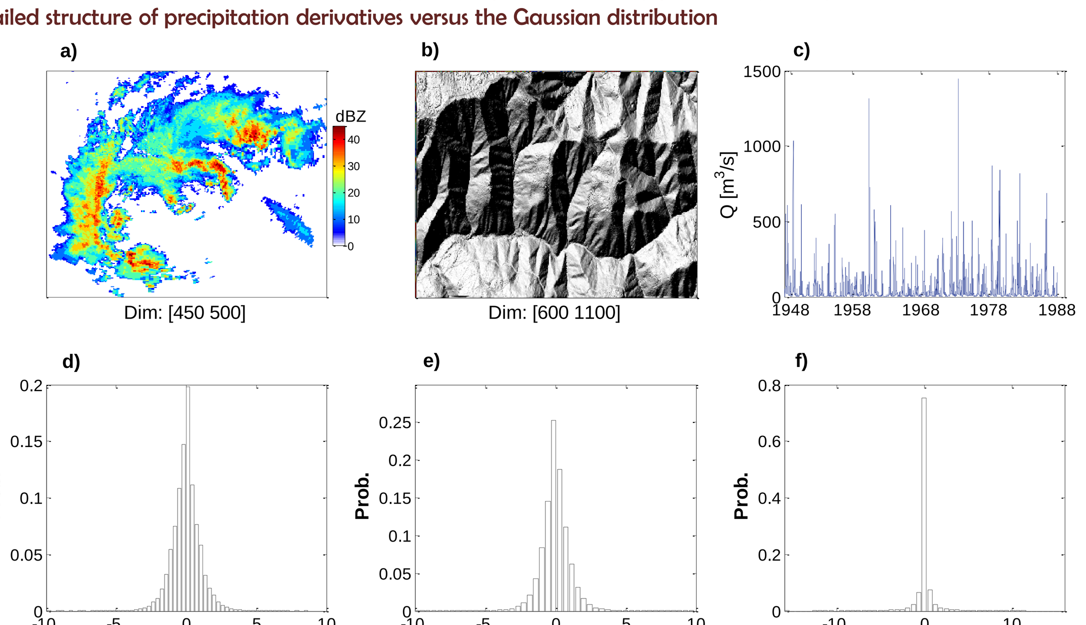

Fig.3: Sparsity of some geophysical signals, top panel from left to right: (a) a level III NEXRAD rainfall reflectivity image in dBZ, over Texas on 1999/03/29 (20:13:00 UTC) at resolution 1×1 km; (b) hillshade representation of high resolution lidar topographic data of a small watershed (2.8 km² area) in the Oregon coast range near Coos Bay at resolution 2×2 m; and (c) 40 years of daily streamflow signal (1948-1988) of Leaf river basin at Collins station (1944 km² draining area), Mississippi. The bottom panels from left to right (d)-to-(f), show the corresponding probability histograms of the standardized wavelet coefficients in a probability scale.

New Estimation Paradigms in Downscaling, Fusion, and Assimilation with Sparse Prior

❑ Problem Statement

- **VarDS Problem:** To obtain a high-resolution estimate of the true state ($\mathbf{x}\in\mathbb{R}^m$) from a single noisy and down-sampled observation ($\mathbf{y}\in\mathbb{R}^n$), via a linear observation model, where $m \gg n$. The weighted least squares (WLS) solution for the downscaling problem is not unique (Uniqueness) as there are more unknowns than the equations.

$$\mathbf{y}=\mathbf{Hx}+\mathbf{v} \qquad \mathbf{v}\sim\mathcal{N}(0,\mathbf{R})$$

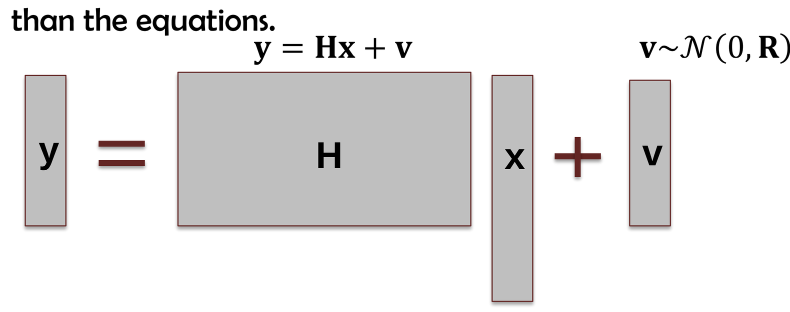

Classic Formulation:

$$\hat{\mathbf{x}} = \operatorname{argmin}_{\mathbf{x}}\left\{\frac{1}{2}\|\mathbf{y}-\mathbf{Hx}\|^2_{\mathbf{R}^{-1}}\right\} \qquad \text{ill-posed !}$$

Regularized Formulation:

$$\hat{\mathbf{x}} = \operatorname{argmin}_{\mathbf{x}}\left\{\frac{1}{2}\|\mathbf{y}-\mathbf{Hx}\|^2_{\mathbf{R}^{-1}} + \lambda\,\|\mathbf{Lx}\|_1\right\}$$

- **VarDF Problem:** To obtain a high-resolution estimate of the true state ($\mathbf{x}\in\mathbb{R}^m$) from a series of noisy and down-sampled observations ($\mathbf{y}^i\in\mathbb{R}^{n_i}$), via a linear observation model, where $\Sigma n^i \gg m$. The weighted least squares (WLS) solution for the data fusion problem is unique (Uniqueness) as the system of equation is over-determined; however, is very sensitive to observation noise (Stability).

$$\mathbf{y}^i=\mathbf{H}^i\mathbf{x}+\mathbf{v}^i \qquad \mathbf{v}\sim\mathcal{N}(0,\mathbf{R}^i)$$

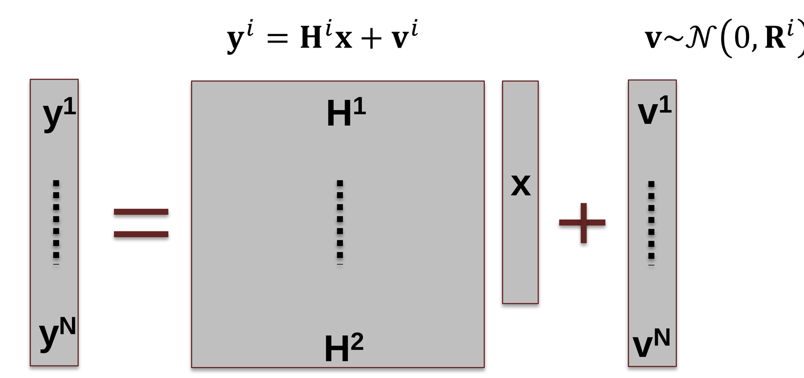

Classic Formulation:

$$\hat{\mathbf{x}} = \operatorname{argmin}_{\mathbf{x}}\left\{\sum_{i=1}^{N}\frac{1}{2}\left(\|\mathbf{y}^i-\mathbf{H}^i\mathbf{x}\|^2_{(\mathbf{R}^i)^{-1}}\right)\right\}$$

Regularized Formulation:

$$\hat{\mathbf{x}} = \operatorname{argmin}_{\mathbf{x}}\left\{\sum_{i=1}^{N}\frac{1}{2}\left(\|\mathbf{y}^i-\mathbf{H}^i\mathbf{x}\|^2_{(\mathbf{R}^i)^{-1}}\right)+\lambda\|\mathbf{Lx}\|_1\right\}$$

- **VarDA Problem :** To obtain a high-resolution estimate of the true initial condition ($\mathbf{x}\in\mathbb{R}^m$) from a series of noisy and down-sampled observations ($\mathbf{y}^i\in\mathbb{R}^{n_i}$) and background state ($\mathbf{x}^b\in\mathbb{R}^m$), which is typically the forecast from the previous time step. The DA problem is also over-determined as the number of equations are more than the unknowns and has a unique solution in a linear setting.

$$\mathbf{y}^i=\mathbf{H}^i\mathbf{x}+\mathbf{v}^i \qquad \mathbf{v}\sim\mathcal{N}(0,\mathbf{R}^i)$$
$$\mathbf{x}^b=\mathbf{x}+\mathbf{w} \qquad \mathbf{w}\sim\mathcal{N}(0,\mathbf{B})$$

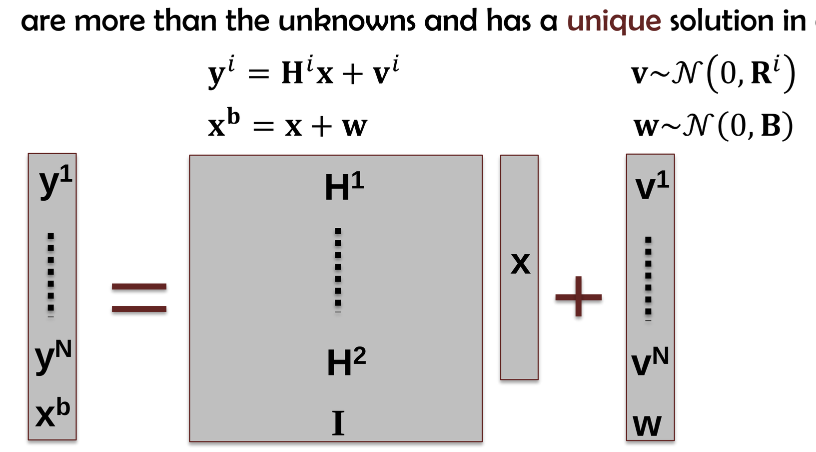

Classic Formulation:

$$\hat{\mathbf{x}} = \operatorname{argmin}_{\mathbf{x}}\left\{\sum_{i=1}^{N}\frac{1}{2}\left(\|\mathbf{y}^i-\mathbf{H}^i\mathbf{x}\|^2_{(\mathbf{R}^i)^{-1}}\right)+\|\mathbf{x}^b-\mathbf{x}\|^2_{\mathbf{B}^{-1}}\right\}$$

Regularized Formulation:

$$\hat{\mathbf{x}} = \operatorname{argmin}_{\mathbf{x}}\left\{\sum_{i=1}^{N}\frac{1}{2}\left(\|\mathbf{y}^i-\mathbf{H}^i\mathbf{x}\|^2_{(\mathbf{R}^i)^{-1}}\right)+\|\mathbf{x}^b-\mathbf{x}\|^2_{\mathbf{B}^{-1}}+\lambda\|\mathbf{Lx}\|_1\right\}$$

- **Statistical Interpretation:** The classic weighted least squares solutions can be interpreted as the Maximum Likelihood (ML) estimator and the regularized formulations are the Maximum a posteriori Estimator (MAP).

$$\hat{\mathbf{x}}_{ML} = \operatorname{argmax}_{\mathbf{x}}\, p(\mathbf{y}|\mathbf{x}) = \operatorname{argmin}_{\mathbf{x}}\{-\log p(\mathbf{y}|\mathbf{x})\} = \operatorname{argmin}_{\mathbf{x}}\left\{\frac{1}{2}(\mathbf{y}-\mathbf{Hx})^T\mathbf{R}^{-1}(\mathbf{y}-\mathbf{Hx})\right\} = \operatorname{argmin}_{\mathbf{x}}\left\{\frac{1}{2}\|\mathbf{y}-\mathbf{Hx}\|^2_{\mathbf{R}^{-1}}\right\}$$

$$\hat{\mathbf{x}}_{MAP} = \operatorname{argmax}_{\mathbf{x}}\, p(\mathbf{x}|\mathbf{y}) = \operatorname{argmin}_{\mathbf{x}}\{-\log p(\mathbf{y}|\mathbf{x}) - \log p(\mathbf{x})\} = \operatorname{argmin}_{\mathbf{x}}\left\{\frac{1}{2}\|\mathbf{y}-\mathbf{Hx}\|^2_{\mathbf{R}^{-1}}+\lambda\|\mathbf{Lx}\|_1\right\}$$

❑ Results on Rainfall VarDS

- The variational downscaling method, using the l1-regularization, is examined to enhance resolution of rainfall reflectivity images. To synthetically produce coarse scale observations, the rainfall images at resolution 1×1 km are coarse grained with an average filter of size 4×4 and 8×8. Relative to the standard deviation of the rainfall fields a small amount of noise (i.e., standard deviation of 1e-3) is also added to resemble observation noise.

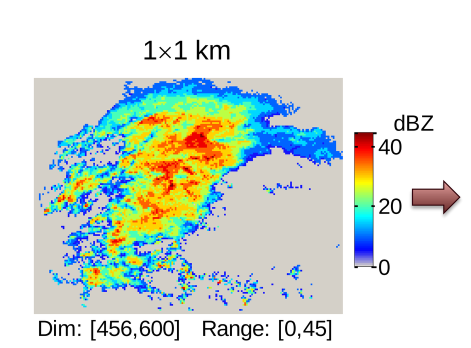

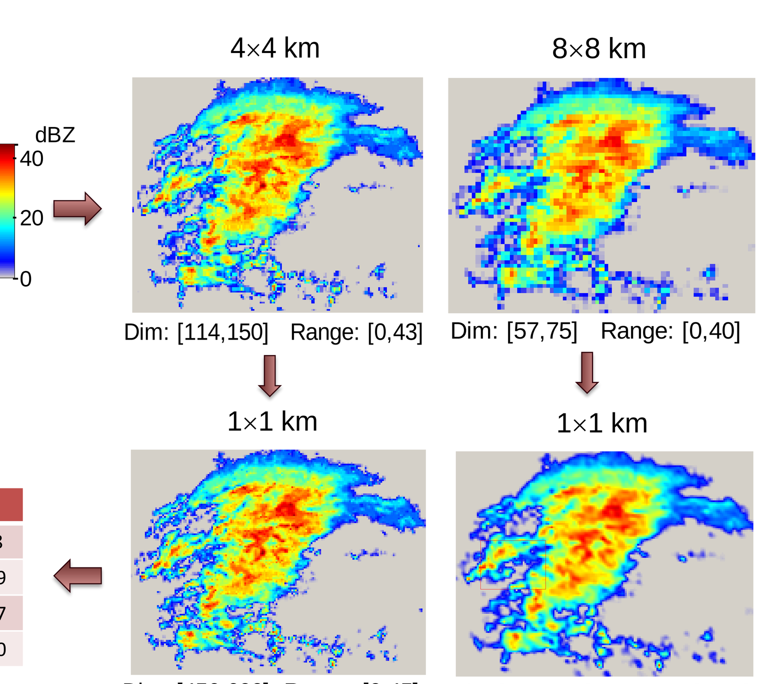

Metric	Observations		VarDs	
(km)	4X4	8x8	4X4	8x8
RMSE	0.19	0.29	0.14	0.19
MAE	0.15	0.25	0.11	0.17
PSNR	23.8	19.6	27.0	24.0

Fig.5: Results of the variation rainfall DS, using l1-regularization. The main advantages compared to stochastic interpolators are: (1) the downscaled field is unique with reduced estimation error; (2) the method is robust to measurement noise; (3) the solution is free of the blockiness. $\mathbf{RMSE} = \|\mathbf{x}-\hat{\mathbf{x}}\|_2/\|\mathbf{x}\|_2$; $\mathbf{RMSE} = \|\mathbf{x}-\hat{\mathbf{x}}\|_1/\|\mathbf{x}\|_1$; $\mathbf{PSNR} = 20\log(\max(\hat{\mathbf{x}})\,/std(\mathbf{x}-\hat{\mathbf{x}}))$.

❑ Results on Rainfall VarDF

- It has been long understood that multiple sources of rainfall observations are highly corrupted with observation error. Figure 6 shows a snapshot of the Hurricane Claudette 07-15-2003 at UTC 11:51:00 observed coincidentally with the TRMM and ground-based NXRAD over Texas-United States. The cross section A-A shows the fact that how much the products of TRMM-PR, TMI and NEXRAD might be different, which necessitates the need for developing robust and practical rainfall fusion algorithms.

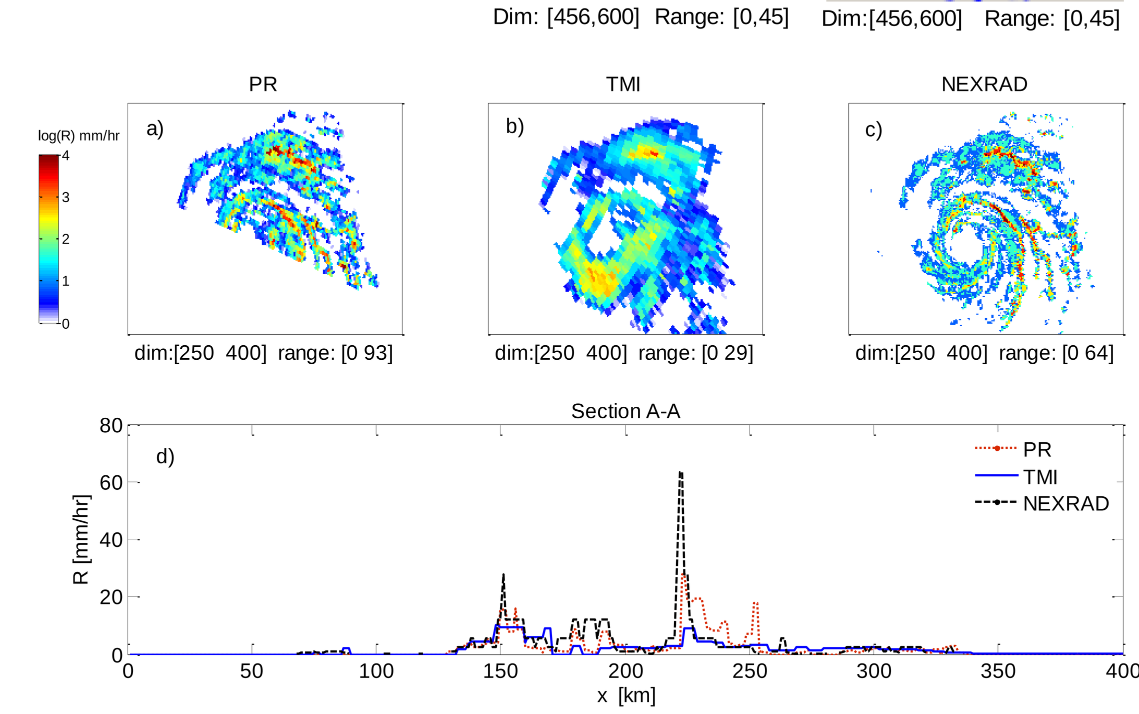

Fig.6: (a) TRMM-PR (2A-25) surface rain of the hurricane Claudette 07-15-2003 at UTC 11:51:00; (b) TMI (2A-12) surface rain rate, (c) ground based NEXRAD observations using convective $Z = 300\mathrm{R}^{1.4}$, (d) the cross-section A-A. It is clear that the TRMM products are severely underestimating the rain rate compared to the ground-based observations.

Results

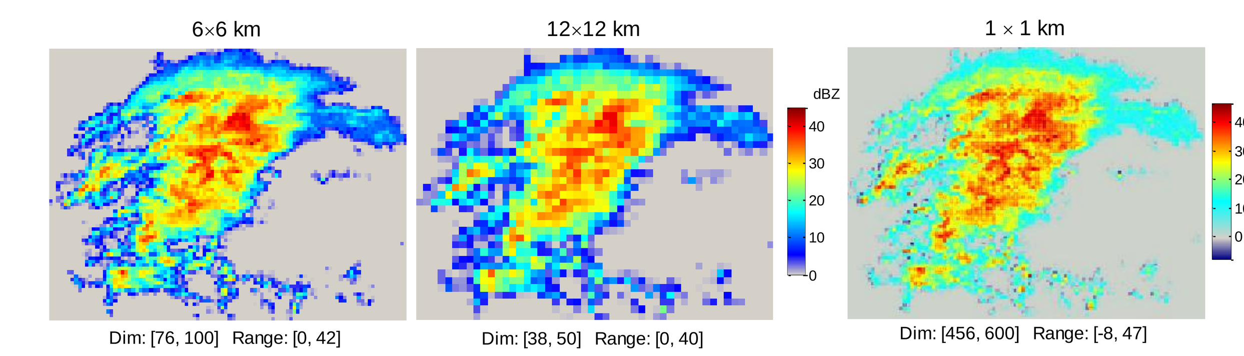

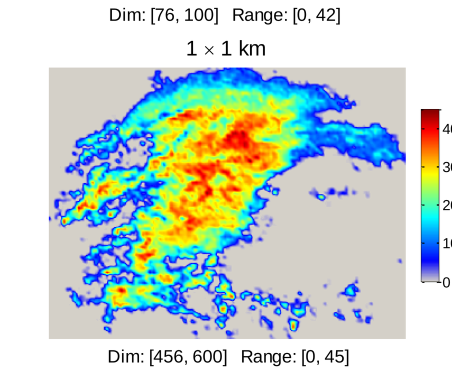

Metric	Observations		DsF
(km)	6X6	12x12	1x1
RMSE	0.25	0.35	0.17
MAE	0.21	0.32	0.15
PSNR	21.3	18.1	25.0

Fig.7: Results of the variational VarDF, using the l1-regularization for fusing multi-sensor remotely sensed rainfall reflectivity fields. (a-b) Reconstructed low-resolution and noisy rainfall observations at scales of 6 and 12 km in grid spacing. (c) The results of the WLS solution, and (d) the solution of the l1-regularized with $\lambda = 1e-3$.

❑ Regularized VarDA in spectral domains using linear advection-diffusion equation

- **4D-VAR:** The promise of the proposed regularized 4D-VAR data assimilation methodology, is shown via assimilating noisy observations into the dynamics of the heat equation with top-hat initial condition.

$$\mathbf{x}_t(s,t) + a\,\mathbf{x}_s(s,t) = \epsilon\,\mathbf{x}_{ss}(s,t)$$
$$\mathbf{x}(s,0) = \mathbf{x}_0(s)$$

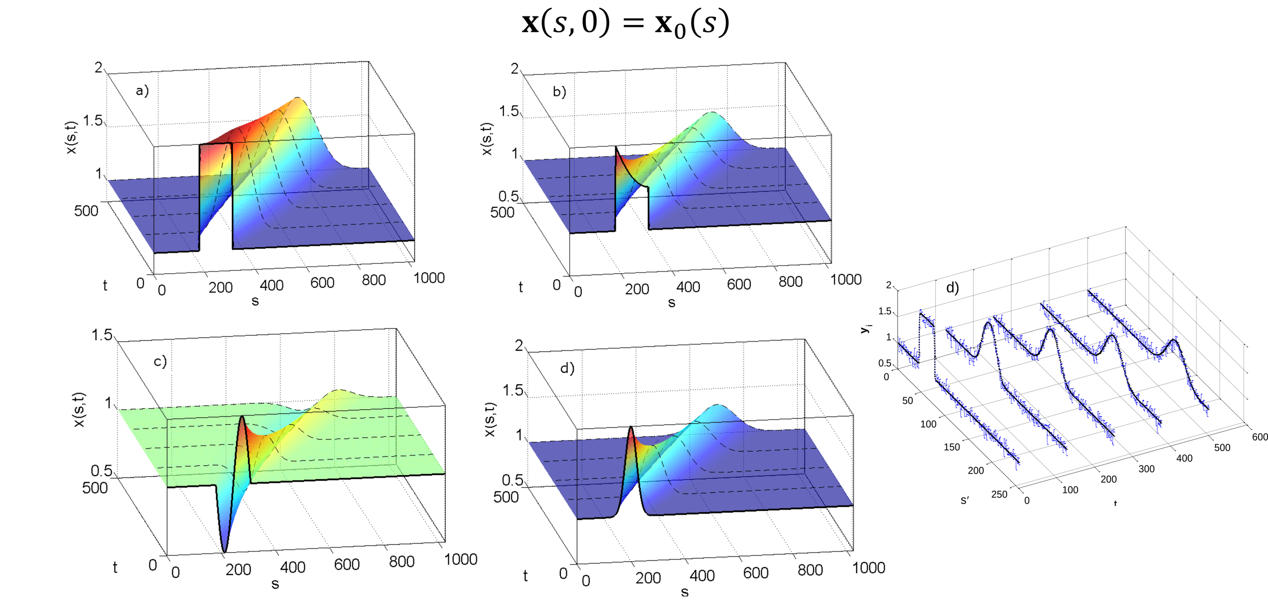

Fig.8: (a) flat top-hat, (b) quadratic top-hat, (c) periodic sinusoidal, and (d) square-exponential initial conditions and a 1D sample of the available downsampled and noisy observations in the 4D-VAR. The first two in (a) and (b) exhibit sparse representation in the wavelet domain while the next two initial conditions show sparse representation in the discrete cosine domain (DCT). Initial conditions are evolved under the model equation with $\epsilon = 4\,[\mathrm{L}^2/\mathrm{T}]$, while the broken lines show the time instants where the low-resolution and noisy observations become available.

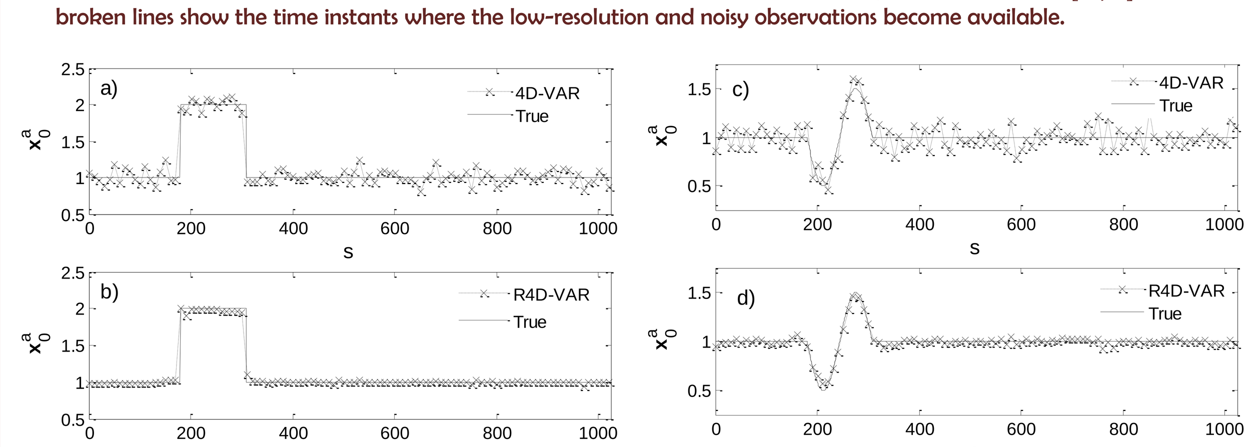

Fig.9: compares the results of the classic and ℓ_1-norm RVDA in a 4D-VAR setting. (a-b) results of the classic 4D-VAR and (c-d) results of the ℓ_1 regularized 4D-VAR.

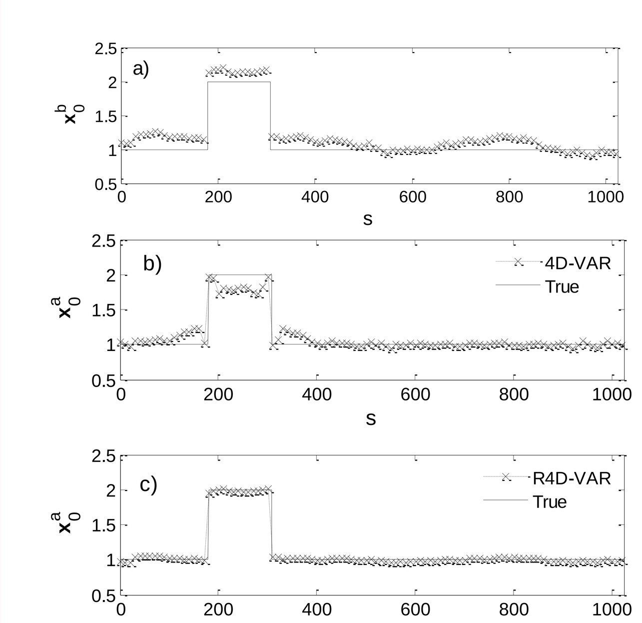

White Background Error ($\mathbf{B}\cong 0.08\,\mathbf{I}$; $\mathbf{R}\cong 0.10\,\mathbf{I}$)			
	IC-1, κ (B) = 1		
	MSE	MAE	BIAS
R4D-VAR	0.019	0.0099	0.0016
4D-VAR	0.070	0.0590	0.00044
	IC-2 κ (B) = 1		
R4D-VAR	0.030	0.023	0.0038
4D-VAR	0.096	0.077	0.0022
Correlated Background Error ($\mathbf{B}\cong 0.08\,\mathbf{C_B}$; $\mathbf{R}\cong 0.10\,\mathbf{I}$)			
	IC-1 κ (B)~10^5		
R4D-VAR	0.022	0.019	0.0035
4D-VAR	0.086	0.054	0.0011

Fig.10: compares the results of the classic and ℓ_1-norm RVDA in a 4D-VAR setting, while the background error is severely ill-conditioned.

Acknowledgments

This research is supported by : NASA-NNX07AD33G; NESSF fellowship (2012-2013); a U of M Doctoral Dissertation Fellowship.

Publications:

1- Ebtehaj, M., and E. Foufoula-Georgiou (2010), " Orographic Signature on Multiscale Statistics of Extreme Rainfall: A Storm Scale Study ", JGR (A)
2- Ebtehaj, A.M., and E. Foufoula-Georgiou (2011), " Statistics of Precipitation Images and Cascade of GSM in the Wavelet Domain ", JGR(A)
3- Ebtehaj, A.M., E. Foufoula-Georgiou (2011), " Adaptive non-Gaussian Fusion of Multi-sensor precipitation in the wavelet domain "JGR(A)
4- Ebtehaj A.M., E. Foufoula Georgiou. G. Lerman (2012), Sparse Precipitation Downscaling , JGR(A)
5- Ebtehaj A.M., E. Foufoula Georgiou (2012) "Variational downscaling, Fusion and Assimilation of Hydrometeorological states via regularization", WRR , accepted